Structural Safety and Reliability, Shiraishi, Shinozuka & Wen (eds) © 1998 Balkema, Rotterdam, ISBN 90 5410 978 5

Engineering simulation of ground motions using a seismological model

T.Ohsumi & H.Darama
Planning and Research Department, Research and Development Center, Nippon Koei Co. Ltd, Takasaki, Ibaraki, Japan
T.Harada
Department of Civil Engineering, Miyazaki University, Japan

ABSTRACT:This paper describes a digital simulation method of ground motions using a seismological model. The method is based on the spectral representation of stochastic waves in conjunction with the stochastic summation of the small ruptures in making use of the representation theorem of elastodynamics of the far field seismic waves. Numerical example demonstrates the effect of the directivity of seismic waves on the acceleration time histories.

1 INTRODUCTION

In order to simulate high frequency ground motions ($\geq$ about 1 Hz) at an average site from an average earthquake of specified size, Boore (1983) presented a stochastic method in which the Fourier spectrum amplitude of simulated ground motion approximates the acceleration spectrum with ω^{-2} property and a single corner frequency (Hanks and McGuire, 1981).

It is well known that the rupture plane of large earthquake is too large to be treated as a point source, and the slip motion as well as stress drop are not uniform (irregular) over the extended rupture plane. These heterogeneities of the rupture process may cause the significant departure from the self similar ω^{-2} model of source spectrum (Aki and Richards,1980; Papageorgiou,1988).

In order to represent a type of heterogeneity of the extended rupture, the effects of source-station geometry, and the effects of propagating rupture in a simple model, Joyner and Boore (1986) considered a model where many small rupture areas are added together with their start times distributed randomly with uniform probability over the rupture duration.

In this paper, we apply the above Joyner and Boore method to the general empirical Green's function method proposed by Harada, *et al.*(1995, 1996) which is the generalization of the Irikura formulation (Irikura, 1988). Consequently, we propose an average spectrum of ground motions at a distance from an extended rupture where a type of heterogeneity of the extended rupture, the effects of source-station geometry, and the effects of propagating rupture are taken into account.

2 SPECTRUM OF GROUND MOTION FROM STOCHASTIC SUMMATION OF SMALL EARTHQUAKES

2.1 *Starting Equations*

The starting equations in this paper belong to the empirical Green's function method initially suggested by Hartzell (1978). This method, which has been discussed in detail by Irikura (1988), is a method to simulate ground motions from an extended rupture on the basis of the representation theorem of elastodynamics. Here, a brief discussion of the relevant mathematical formulation is presented in the frequency domain, and a new transfer function is presented, which accounts for the difference of the slip time functions between extended rupture and small rupture area.

The extended rupture plane with length L and width W is divided into small rupture areas with length ΔL and width ΔW, as shown in Fig.1. Using the representation theorem of elastodynamics, the far-field displacement $\boldsymbol{u}(\boldsymbol{x},t)$ in a homogeneous, isotropic, and layered medium can be expressed in the following integral form (Aki and

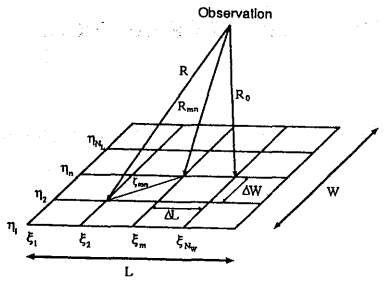

Fig.1 Schematic diagram of the Green's function method and its notation

Richards, 1980; Somerville,*et al.*, 1991):

$$\boldsymbol{u}(\boldsymbol{x},t)=\sum_{m=1}^{N_L}\sum_{n=1}^{N_W}\int_{\xi_m}^{\xi_m+\Delta L}\int_{\eta_n}^{\eta_n+\Delta W}\dot{D}(\xi_m,\eta_n,t-\tau_{mn}) *\boldsymbol{G}(\boldsymbol{x},\xi_m,\eta_n,t-t_{mn})d\xi d\eta \qquad (2.1)$$

where $\boldsymbol{x}=(x,y,z)^T$ is the observation station, $\dot{D}(\xi,\eta,t)$ is the velocity of the source time function at position (ξ,η) on the extended rupture, $\boldsymbol{G}(\boldsymbol{x},\xi,\eta,t-t_{\xi\eta})$ is the Green's function (the impulse response of medium), and $*$ represents a convolution. τ_{mn} is the rupture propagation time from the hypocenter of extended rupture to the $(m,n)^{th}$ small rupture area, and t_{mn} is the propagation time for S waves to travel from the $(m,n)^{th}$ small rupture area to the observation station, which are defined by:

$$\tau_{mn}=\frac{\zeta_{mn}}{V_R};\quad t_{mn}=\frac{R_{mn}-R}{C_S} \qquad (2.2)$$

where ζ_{mn} is the distance from the hypocenter of the extended rupture to the $(m,n)^{th}$ small rupture area, R_{mn} is the distance from the $(m,n)^{th}$ area to the observation station, R is the hypocentral distance of the extended rupture, V_R is the rupture velocity, and C_S the S wave velocity of the medium.

The Fourier transform of Eq.(2.1) yields the following equation:

$$\boldsymbol{u}(\boldsymbol{x},\omega)=\sum_{m=1}^{N_L}\sum_{n=1}^{N_W}\int_{\xi_m}^{\xi_m+\Delta L}\int_{\eta_n}^{\eta_n+\Delta W}\dot{D}(\xi_m,\eta_n,\omega) \boldsymbol{G}(\boldsymbol{x},\xi_m,\eta_n,\omega)e^{-i\omega(\tau_{mn}+t_{mn})}d\xi d\eta \qquad (2.3)$$

In order to take into account the difference of the slip time functions between the extended rupture and the small rupture, the transfer function is introduced, which is defined as:

$$T_{mn}(\omega)=\frac{\dot{D}(\xi_m,\eta_n,\omega)}{\dot{D}_{mn}(\xi_m,\eta_n,\omega)} \qquad (2.4)$$

where $\dot{D}_{mn}(\xi_m,\eta_n,\omega)$ is the Fourier transform of the velocity of the slip time function at position (ξ_m,η_n) of the small rupture. By using Eq.(2.4), Eq.(2.3) can be written as:

$$\boldsymbol{u}(\boldsymbol{x},\omega)=\sum_{m=1}^{N_L}\sum_{n=1}^{N_W}T_{mn}(\omega)\boldsymbol{u}_{mn}(\boldsymbol{x},\omega) \qquad (2.5a)$$

where

$$\boldsymbol{u}_{mn}(\boldsymbol{x},\omega)=\int_{\xi_m}^{\xi_m+\Delta L}\int_{\eta_n}^{\eta_n+\Delta W}\dot{D}_{mn}(\xi_m,\eta_n,\omega) \boldsymbol{G}(\boldsymbol{x},\xi_m,\eta_n,\omega)e^{-i\omega(\tau_{mn}+t_{mn})}d\xi d\eta \qquad (2.5b)$$

In Eq.(2.5b), $\boldsymbol{u}_{mn}(\boldsymbol{x},\omega)$ is the far-field displacement due to the small rupture. Equation (2.5) indicates that the motions from the extended rupture is the summation of the motions from the $N_L\times N_W$ small rupture areas with the weight of $T_{mn}(\omega)$.

Based on Eq.(2.5), an approximate method can be obtained, using a single record $\boldsymbol{u}_0(\boldsymbol{x},\omega)$ due to the $(m_0,n_0)^{th}$ rupture area. By assuming that the slip time function of each small rupture and the Green's function from the position of each small rupture to the observation station are approximately equal to those from the $(m_0,n_0)^{th}$ rupture area, then Eq.(2.5a) can be reduced as:

$$\boldsymbol{u}(\boldsymbol{x},\omega)=\sum_{m=1}^{N_L}\sum_{n=1}^{N_W}\frac{R_0}{R_{mn}}T_{mn}(\omega)e^{-i\omega\tilde{t}_{mn}}\boldsymbol{u}_0(\boldsymbol{x},\omega) \qquad (2.6a)$$

where

$$\tilde{t}_{mn}=\tau_{mn}+t_{mn} \qquad (2.6b)$$

In deriving Eq.(2.6) the effect of the hypocentral distance on the Green's function has been considered approximately because the S wave attenuates inversely proportional to the hypocentral distance in a homogeneous isotropic medium.

From the similarity conditions of earthquakes (Kanamori *et al.*, 1975), the following relations are derived:

$$\left(\frac{M_0}{m_0}\right)^{1/3}=\frac{L}{\Delta L}=\frac{W}{\Delta W}=\frac{D}{D_0}=\frac{\tau}{\tau_0}=N \qquad (2.7)$$

where $N=N_L=N_W$, and M_0 is the seismic moment of the extended rupture; m_0 the seismic moment of the small rupture area; D and τ are the final offset of the dislocation and the dislocation rise time of the extended rupture, respectively; D_0 and τ_0 those of the small rupture.

The transfer function $T_{mn}(\omega)$ defined by Eq.(2.4)

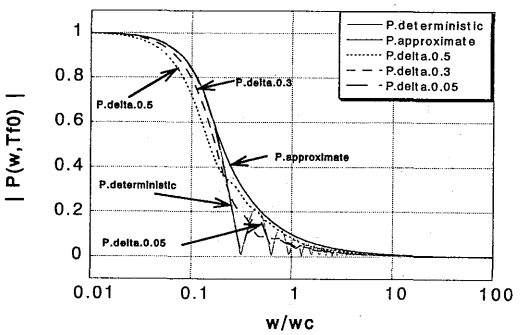

Fig.2 Frequency variation of $|P(\omega, T_f)|$

can be obtained by specifying a slip time function. The following transfer function is used in this paper:

$$T_{mn}(\omega) = \left[\frac{i\omega + \frac{N}{\tau}}{i\omega + \frac{1}{\tau}}\right]\left[\frac{1+\kappa(\frac{\omega\tau}{2})^2}{1+(\frac{\omega\tau}{2})^2}\right] \qquad (2.8)$$

where κ is a parameter that controls the value of the transfer function in high frequency range($\omega \geq \omega_c = 2/\tau$). Although several physical models exist (Aki and Richards, 1980), the generation process of high frequency seismic waves due to extended rupture may be quite complex. Therefore, without the use of physical models, one parameter κ has been introduced here, which has to be empirically estimated. For κ=1, the transfer function is equivalent to that obtained by assuming the exponential function for slip time functions of the extended and small rupture areas (Harada *et al.*, 1995).

2.2*Average characteristics of the source spectrum of an extended rupture obtained from a stochastic summation of small rupture areas*

We consider here a simple model for a simulation of the many patterns of irregular propagation of a coherent rupture front from a specified hypocenter on a given extented rupture plane. For each pattern of irregular ruptures, the small rupture areas can be considered to be distributed on the extented rupture plane with later start times at progressively greater distances from the hypocenter. However, in considering the collection of many patterns it may be appropriate to assume approximately that the start times of small rupture areas are randomly distributed with uniform probability over the observed rupture duration T_f of the given extended rupture. It is noted here that the duration T_f depends on the size of the extended rupture and on the rupture velocity, but it also depends on the orientation of the observation relative to the rupture (see subsection 2.3). It is also noted that the duration T_f is assumed to be a random variable with uniform probability. By considering the practical situation, the small rupture areas are assumed identical. For the attention of the source characteristics, we neglect the correction of the hypocentral distance.

With the above assumptions the Fourier spectrum of the uni- component waveform $u_S(\omega)$ from the extended rupture may be written such as:

$$u_S(\omega) = \left[\sum_{m=1}^{N}\sum_{n=1}^{N} T_{mn}(\omega) e^{-i\omega t^*_{mn}}\right] u_{S0}(\omega) \qquad (2.9)$$

where $u_{S0}(\omega)$ represents the Fourier spectrum of the uni-component waveform from a small rupture area, and t^*_{mn} the time delay uniformly distributed over T_f. By taking the expectation over the ensemble, the average source spectrum $|u_S(\omega)|$ is obtained as:

$$|u_S(\omega)| = SUM_N(\omega)|T(\omega)||u_{S0}(\omega)| \qquad (2.10)$$

where $|T(\omega)|$=$|T_{mn}(\omega)|$, and SUM_N (ω) is the coefficient of random summation given by:

$$SUM_N(\omega) = \left[N^2\left\{1+(N^2-1)|P(\omega,T_{f0})|^2\right\}\right]^{1/2} \qquad (2.11a)$$

where

$$|P(\omega,T_{f0})| = \frac{1}{4\sqrt{3}\delta_{Tf}\left(\frac{\omega}{\omega_{f0}}\right)}\Big[(\mathrm{Si}[\varpi_1]-\mathrm{Si}[\varpi_2])^2 + (\mathrm{Ci}[\varpi_1]-\mathrm{Ci}[\varpi_2]-\ln[\varpi_1]+\ln[\varpi_2])^2\Big]^{1/2} \qquad (2.11b)$$

where

$$\varpi_1 = 2(1+\sqrt{3}\delta_{Tf}\frac{\omega}{\omega_{f0}}) \qquad (2.11c)$$

$$\varpi_2 = 2(1-\sqrt{3}\delta_{Tf}\frac{\omega}{\omega_{f0}}) \qquad (2.11d)$$

In Eq.(2.11a) T_{f0} is the mean of the observed rupture duration T_f, and δ_{Tf} is the coefficient of variation of T_f. The functions Si and Ci represent the sine and cosine integrals. The first corner frequency ω_{f0} is defined in this study such as:

$$\omega_{f0} = \frac{2}{T_{f0}} \qquad (2.11e)$$

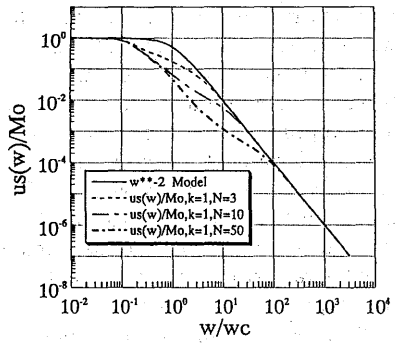

Fig.3 Normalized spectra of large earthquake by the Joyner and Boore stochastic summation of small earthquakes, compared to the ω^{-2} spectrum (heavy line). (In the case of $\kappa = 1$)

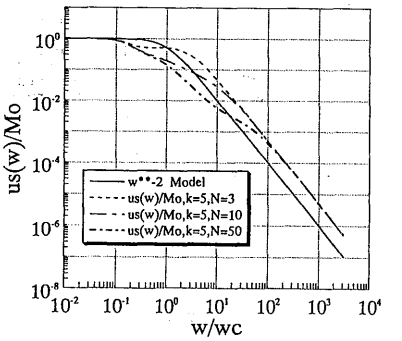

Fig.4 Normalized spectra of large earthquake by the Joyner and Boore stochastic summation of small earthquakes, compared to the ω^{-2} spectrum (heavy line). (In the case of $\kappa = 5$)

The frequency variation of function $|P(\omega, T_{f0})|$ is shown in Fig.2 for δ_{Tf} =0.05, 0.3, and 0.5. For small value of δ_{Tf} =0.05, the frequency variation of $|P(\omega, T_{f0})|$ indicates a wavy form with peaks and troughs, similar to the behavior in the case of deterministic rupture duration ($\delta_{Tf} = 0$) where the function $P(\omega, T_{f0})$ is given by:

$$|P(\omega, T_{f0} = T_f)| = \left| \frac{\sin \dfrac{\omega}{\omega_f}}{\dfrac{\omega}{\omega_f}} \right| \qquad (2.12)$$

The function of Eq.(2.12) is the same derived by Joyner and Boore (1986), and also shown in Fig.2. For large value of δ_{Tf}=0.5, the frequency variation of $|P(\omega, T_{f0})|$ is smooth. By considering the fact that the variation in the first corner frequency ω_{f0} may be large, we propose the following simple function for $|P(\omega, T_{f0})|$:

$$|P(\omega, T_{f0})| = \begin{cases} 1 - c_1 \left(\dfrac{\omega}{\omega_{f0}}\right)^2 + c_2 \left(\dfrac{\omega}{\omega_{f0}}\right)^4 & 0 \le \dfrac{\omega}{\omega_{f0}} \le \dfrac{\pi}{2} \\ \dfrac{1}{\dfrac{\omega}{\omega_{f0}}} & \dfrac{\pi}{2} \le \dfrac{\omega}{\omega_{f0}} \end{cases} \qquad (2.13)$$

where c_1=0.16605, and c_2=0.00761. The function of Eq.(2.13) is also shown in Fig.2.

By introducing the second and third corner frequencies defined by,

$$\omega_c = \frac{2}{\tau}, \qquad \omega_{c0} = \frac{2}{\tau_0} \qquad (2.14)$$

the transfer function of Eq.(2.8) can be rewritten as:

$$T(\omega) = T_{mn}(\omega) = \left[\frac{N + i(2\dfrac{\omega}{\omega_c})}{1 + i(2\dfrac{\omega}{\omega_c})} \right] \left[\frac{1 + \kappa(\dfrac{\omega}{\omega_c})^2}{1 + (\dfrac{\omega}{\omega_c})^2} \right] \qquad (2.15a)$$

where,

$$N = (\frac{M_0}{m_0})^{1/3} = \frac{\omega_{c0}}{\omega_c} \qquad (2.15b)$$

The source spectrum of the small rupture is assumed to be ω^{-2} model such as:

$$|u_0(\omega)| = \frac{m_0}{1 + (\dfrac{\omega}{N\omega_c})^2} \qquad (2.16)$$

In the two extreme frequencies where $\omega \to 0$ and $\omega \to \infty$, the source spectrum of an extended rupture is found from Eq.(2.10) to be given by:

$$|u_S(\omega)| = \begin{cases} N^3 m_0 = M_0 & \omega \to 0 \\ \kappa M_0 \left(\dfrac{\omega_c}{\omega}\right)^2 & \omega \to \infty \end{cases} \qquad (2.17)$$

Figures 3 and 4 show the average source spectra of extended rupture normalized by the seismic moment M_0 for the cases of κ=1 and 5, respectively. In each figure, ω_{f0}/ω_c =1/10 is assumed and the variations with the summation parameter N are shown. For comparison, the ω^{-2} source spectrum model with the second corner frequency ω_c is shown by the heavy line in each figure. It is found from Fig.3 (for the case of κ =1) that the source spectrum of extended rupture follows the ω^{-2} model at the lower frequency (ω_{f0}) and the

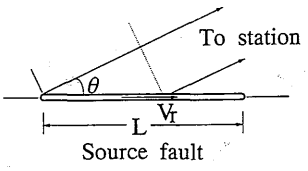

Fig.5 Geometry of a rupturing fault and the path to an observation station

higher frequency (ω_{c0}) ranges, but at intermediate frequency range its spectral amplitude is lower as the summation parameter N increases than that expected from the ω^{-2} model. These characteristics observed from Fig.3 are also observed from Fig.4 (for the case of κ=5), but the source spectral amplitude is amplified by a factor of κ at higher frequency range ($\omega \geq \omega_{c0}$).

By comparing these characteristics shown in Figs. 3 and 4 with those obtained from the various irregular source models (for examples, Izutani, 1984; Papageorgiou, 1988) where the heterogeneity of either slip or stress drop on the extended rupture plane is taken into account, the parameter κ may be found to be equivalent to the ratio of local stress drop to global stress drop or the ratio of dynamic stress drop to static stress drop.

2.3 *Average rupture duration observed at a station*

The observed rupture duration T_f depends on the size of the extended rupture and the rupture velocity, but it also depends on the orientation of the observation station relative to the extended rupture. For simplicity we adopt the simplest model for the geometry of a rupture and the path to an observation station as shown in Fig.5. The observed rupture duration ($R \gg L$ where R is the hypocentral distance and L is the strike length of the extended rupture) is given such as (Ben-Menahem, 1961):

$$T_f = \frac{L}{V_R}\left(1 - \frac{V_R}{C_S}\cos\theta\right) \qquad (2.18a)$$

where θ is the azimuth angle from the strike of extended rupture to the observation station. V_R and C_S are the rupture velocity and the S wave velocity. In Eq.(2.18a), L, V_R, C_S, and θ may be considered as random variables. However, for simplicity, we use the rupture duration of Eq.(2.18a) as an estimate of the average rupture duration observed at a station:

$$T_{f0} \simeq T_f \qquad (2.18b)$$

3 SAMPLE GROUND MOTION FROM STOCHASTIC SUMMATION OF SMALL EARTHQUAKES

A sample acceleration time history of ground motion is generated using the spectral representation of stochastic waves proposed by Shinozuka (1974); Shinozuka *et al.*(1987). In this method, the power spectrum of ground acceleration have to be given, then the stationary acceleration time history is generated by the following equation:

$$a_s(t) = \sqrt{2}\sum_{j=1}^{N_\omega}\sqrt{2S_{aa}(\omega_j)\Delta\omega}\cos(\omega_j t + \phi_j) \quad (3.1a)$$

where,

$$\omega_j = j\Delta\omega;\ \ \Delta\omega = \frac{\omega_u}{N_\omega};\ \ j = 1, 2, \ldots, N_\omega \quad (3.1b)$$

An upper bound of the frequency ω_u in Eq.(3.1b) represents an upper cut-off frequency beyond which $S_{aa}(\omega_j)$ may be assumed to be zero for either mathematical or physical reasons. In Eq.(3.1a), ϕ_j are independent random phase angles uniformly distributed over the range $(0, 2\pi)$. Note that the simulated time history is asymptotically Gaussian as N_ω becomes large due to the central limit theorem.

The nonstationary acceleration time history $a(t)$ is obtained by multiplying an envelope function $W(t)$ into the stationary time history $a_s(t)$.

$$a(t) = W(t)a_s(t) \qquad (3.2)$$

In this study, the following expression for the envelope function is used:

$$W(t) = \begin{cases} \left(\dfrac{t}{T_b}\right)^2 & 0 \leq t \leq T_b \\ 1 & T_b \leq t \leq T_c \\ \exp[-c(t - T_c)] & T_c \leq t \leq T_d \end{cases} \qquad (3.3)$$

where the duration (effective duration T_e)of the stationary strong portion (T_e =T_c - T_b) of ground motion is assumed equal to the average observed rupture duration in Eq.(2.18).

$$T_e = T_c - T_b = T_{f0} \qquad (3.4a)$$

Then, the duration of nonstationary ground motion (T_d) can be given using the empirical relations by Ohsaki(1994):

$$T_d = 2.63T_{f0} \qquad (3.4b)$$

$$T_b = [0.12 - 0.04(M_{JMA} - 7)]T_d \qquad (3.4c)$$

$$T_c = [0.50 - 0.04(M_{JMA} - 7)]T_d \qquad (3.4d)$$

$$c = -\frac{\ln 0.1}{T_d - T_c} \qquad (3.4e)$$

The power spectrum $S_{aa}(\omega)$ of ground acceleration appearing in Eq.(3.1a) is constructed using the spectrum of chapter 2. Then, $S_{aa}(\omega)$ with the effective duration T_e=T_{f0} is given by:

$$S_{aa}(\omega) = \frac{1}{2\pi T_e}|A(\omega)|^2 \qquad (3.5)$$

where $|A(\omega)|$ is the spectrum of ground acceleration which is given by:

$$|A(\omega)| = SUM_N(\omega)|T(\omega)||A_0(\omega)| \qquad (3.6)$$

where $|A_0(\omega)|$ is the acceleration spectrum of small earthquake observed at a distance R (the hypocenter of a small earthquake is assumed to be the same place of the extended rupture) with seismic moment m_0, which is given by:

$$|A_0(\omega)| = CA_{S0}(\omega)A_D(\omega)A_A(\omega) \qquad (3.7)$$

where C, $A_{S0}(\omega)$, $A_D(\omega)$, and $A_A(\omega)$, represent a scaling factor, a source spectrum, a diminution factor, and a local soil amplification factor, respectively.

The scaling factor and the source spectrum of the small earthquake are given by:

$$C = \frac{R(\theta,\varphi)FV}{4\pi\rho C_S^3};\ A_{S0}(\omega) = \frac{m_0\omega^2}{1+(\omega/\omega_{c0})^2} \qquad (3.8)$$

where $R(\theta,\varphi)$ is the average correction factor for radiation pattern, F accounts for free-surface amplification, V accounts for the partitioning of the energy in two horizontal components, ρ is the density of the material at the source, C_S is the S wave velocity at the source, and ω_{c0} is the corner frequency of the small earthquake.

The diminution factor and the local soil amplification factor are given by:

$$A_D(\omega) = \frac{1}{1+(\omega/\omega_{max})^n}\frac{1}{R}\exp(-\frac{\omega R}{2QC_S}); \qquad (3.9a)$$

$$A_A(\omega) = \sqrt{\frac{\rho C_S}{\rho_0 C_{S0}}}\frac{\sqrt{1+4h_g^2(\frac{\omega}{\omega_g})^2}}{\sqrt{(1-(\frac{\omega}{\omega_g})^2)^2+4h_g^2(\frac{\omega}{\omega_g})^2}} \qquad (3.9b)$$

The first factor in $A_D(\omega)$ is the high-cut filter that accounts for the sudden drop that the spectrum exhibits above ω_{max}. It is assumed here $n = 1$. The second factor is the geometric spreading factor of the S wave. The third factor is the effect of the material damping on wave propagation in which Q is a frequency-dependent attenuation factor.

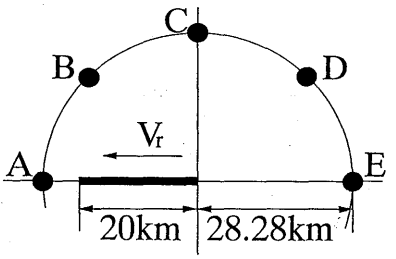

Fig.6 Plane view of the rupturing fault and the 5 stations with equal hypocentral distance

The local soil amplification factor $A_A(\omega)$ is composed of the deep soil amplification from the deep ground level near the source with the density ρ and the S wave velocity C_S to the engineering ground base with ρ_0 and S wave velocity C_{S0} of about 0.5 to 1 km/s, and the shallow soil amplification from the engineering ground base to the ground surface. The first factor in $A_A(\omega)$ of Eq.(3.9b) corresponds to the deep soil amplification factor proposed by Boore (1987), and the second factor to the shallow soil amplification represented by the Kanai-Tajimi spectrum (Kanai, 1957; Tajimi, 1960). ω_g and h_g control the peak position and the peak value of the amplification factor; $\omega_g = 15.6$(rad/sec), $h_g = 0.6$ for a firm soil.

4 NUMERICAL EXAMPLE OF SAMPLE GROUND MOTIONS

Numerical example is given now in order to demonstrate an applicability of the simulation method using a stochastic summation of small earthquakes to an artificial generation of strong motions for aseismic design. The example is also given to visualize the effect of directivity of seismic waves on the ground motions.

In this numerical example, the horizontal ground acceleration time histories on rock site are generated from an earthquake with magnitude M_{JMA} = 7.0 and hypocentral distance R=30 (km). A strike slip fault with length L=20 (km) and width W=10 (km) is considered. The hypocenter is assumed to be at the bottom edge of the the extended rupture area.

The determination of the magnitude of small earthquake may be arbitrary. In this study the magnitude of small earthquake M_{JMA0} is assumed

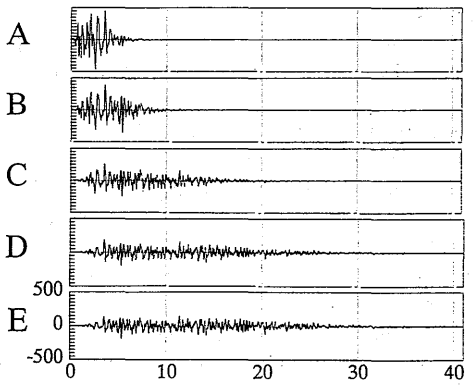

Fig.7 Sample ground acceleration time histories at 5 stations on rock site with equal hypocentral distance (M_{JMA}=7.0, R=30 km)

to be 5.0, because the many empirical relationships in the parameters are usually obtained for the magnitude greater than about 4.0 to 5.0.

We determine the seismic moments of the earthquakes with M_{JMA}=7.0 and M_{JMA0}=5.0 by the following empirical relation which is obtained from the earthquakes occurred under the sea area around Japanese teritory (Sato, 1989):

$$M_0(\text{dyne-cm}) = 10^{(1.5M_{JMA}+16.2)} \qquad (4.1)$$

From Eq.(2.7) the summation parameter N is determiend using the seismic moments, M_0 and m_0, of large and small erthquakes such as:

$$N = (\frac{M_0}{m_0})^{1/3} = 10 \qquad (4.2)$$

In evaluating the acceleration spectrum $|A_{A0}(\omega)|$ of ground motion from small earthquake, the following values are used:

$$R(\theta,\varphi) = 0.63;\ \ F = 2.0;\ \ V = 0.5; \qquad (4.4a)$$

$$\rho = 2.7\text{gr/cm}^3;\ \ C_S = 3.6\text{km/sec}; \qquad (4.4b)$$

$$\omega_{c0} = 9.3\text{rad/sec};\ \ \omega_{max} = 28.7\text{rad/sec} \qquad (4.4c)$$

$$Q = 10^{(q_1 \log(\omega/2\pi) + q_2)} \qquad (4.4d)$$

where q_1=0.64, q_2=2.1.

The soil amplification of deep soil layers is assumed constant as:

$$\sqrt{\frac{\rho C_S}{\rho_0 C_{S0}}} = 2.0 \qquad (4.5a)$$

The soil amplification of shallow soil layers is evaluated using the following parameters:

$$\omega_g = 5.56\text{rad/sec};\ \ h_g = 0.6 \qquad (4.5b)$$

The ground acceleration time histories at 5 stations on rock site in Fig.6 are generated, with time interval Δt =0.01 sec, and $\omega_u = 2\pi \times 50$ rad/sec, N_ω=1024. The sample of acceleration time histories at 5 stations (M_{JMA}=7.0, R= 30km, on rock site) are shown in Fig.7. It is observed from Fig.7 that even in the same hypocentral distance R= 30 (km), the acceleration time histories are quite different from station to station in peak amplitude and duration. The higher acceleration and the shorter duration are observed in the stations A and B which are located in the direction of propagating rupture of the fault, while the lower acceleration and the longer duration in the stations D and E located in the oposite direction of the propagating rupture. The phenomenon observed in Fig.7 is well known as the directivity of seismic waves.

5 CONCLUSIONS

This paper describes a digital simulation method of strong earthquake ground motions using a seismological model. It can be concluded that:

(1) Based on the representation theorem of elastodynamics for the far-field seismic waves in the frequency domain, the Fourier spectrum amplitude of ground acceleration motion from an extended fault is constructed by the stochastic summation of small earthquakes proposed by Joyner and Boore (1986), where the rupture start times of each small earthquake are distributed randomly with uniform probability over the rupture duration which is also random variable with uniform probability.

(2) In the stochastic summation, a new transfer function is introduced which originally takes into account, not only the difference of the slip time functions between the extended rupture and the small rupture, but also the irregular slip motion over a heterogeneous extended rupture plane.

(3) One parameter κ introduced into the new transfer function is found to be equivalent to the ratio of local stress drop to global stress drop or the ratio of dynamic stress drop to static stress drop in the available irregular source models where the heterogeneity of either slip or stress drop on the extended rupture plane is taken into account.

(4) The source spectrum of an extended rupture by the stochastic summation have three corner frequencies, ω_{f0}, ω_c, and ω_{c0} which are related to the observed rupture duration of the extended rupture, the rise time of the extended rupture, and the rise time of the small rupture.

(5) Based on the spectral representation of stochastic waves, the simulation method of the nonstationary ground acceleration time histories is summarized.

(6) Numerical example is given in order to make clear the procedure and the evaluation of the model parameters for the generation of ground acceleration time histories.

(7) Numerical example also demonstrates the effect of the directivity of seismic waves on the acceleration time histories.

ACKNOWLEDGMENT

We thank Messrs. Kurokawa, T. and Shigenaga, M., Students of Miyazaki University, for their help in drawing the figures.

REFERENCES

[1] Aki, K., and Richards, P.G. (1980), *Quantitative Seismology, Vols.I and II*, W.H. Freeman and Company.

[2] Ben-Menahem, A. (1961), Radiation of Seismic Surface Waves from a Finite Moving Source, *Bull. of Seism. Soc. of Am., Vol.51*, pp.401-435.

[3] Boore, D.M. (1983), Stochastic Simulation of High Frequency Ground Motions Based on Seismological Models of the Radiated Spectra, *Bull. of Seism. Soc. of Am., Vol.73*, pp.1865-1894.

[4] Hanks, T.C., and McGuire, R.K. (1981), The Character of High-Frequency Strong Ground Motion, *Bull. of Seism. Soc. of Am., Vol.71*, pp.2071-2095.

[5] Harada, T., and Tanaka, T. (1995a), Digital Simulation of Earthquake Ground Motions using a Seismological Model, *Journal of Structural Mechanics and Earthquake Engineering, JSCE, No.507/I-30*, pp.209-217.

[6] Harada, T., and Tanaka, T. (1995b), Digital Simulation of Ground Motions using Stochastic Green's Function and Its Verification, *Proc. of the 3rd Japan Conference on Structural Safety and Reliability*, November, Tokyo, pp.527-534.

[7] Harada, T., and Tanaka, T. (1996), Engineering Simulation of Ground Motions From an Extended Fault, *Proc. of the 11th World Conference on Earthquake Engineering*,

[8] Hartzell, S.H. (1978), Earthquake Aftershock as Green's Functions, *Geophys. Res. Lett., Vol.5*, pp.5.

[9] Irikura, K. (1988), Prediction of Strong Accelerations Motions using Empirical Green's Function, *Proc. of 7th Japan Earthquake Engineering Symposium*, pp.37-42.

[10] Izutani, Y. (1984), Source Parameters Relevant to Heterogeneity of a Fault Plane, *J. Phys. Earth, Vol.32*, pp.511-529.

[11] Joyner, W.B., and Boore, D.M. (1986), On Simulating Large Earthquakes by Green's Function Addition of Smaller Earthquakes, in *Earthquake Source Mechanics*, Geophysical Monograph 37, Edited by Das, S., Boatwright, J., and Scholz, C.H., American Geophysical Union, Washington, D.C., pp.269-274.

[12] Kanai, K. (1957), A Semi-Empirical Formula for the Seismic Characteristics of the Ground Motions, *Bull. of Earthquake Research Institute, The University of Tokyo, Vol.35*, pp.309-325.

[13] Kanamori, H., and Anderson, D.L. (1975), Theoretical Basis of Some Empirical Relations in Seismology, *Bull. of Seism. Soc. of Am., Vol.65*, pp.1073-1095.

[14] Ohosaki, J. (1994), *Introduction of Spectral Analysis of Earthquake Ground Motions*, Kajima Publication, Tokyo, Japan, pp.199-201.

[15] Papageorgiou, A.S. (1988), On Two Characteristic Frequencies of Acceleration Spectra: Patch Corner Frequency and f_{max}, *Bull. of Seism. Soc. of Am., Vol.78*, pp.509-529.

[16] Sato, R. (1989), *Handbook of Source Parameters of Earthquakes in Japan*, Kajima Publication, Tokyo, Japan, pp.82-92.

[17] Shinozuka, M. (1974), Digital Simulation of Random Processes in Engineering Mechanics with the Aid of FFT Technique, In *Stochastic Problems in Mechanics*, Edited by Ariaratnam, S.T. and Leipholz, H.H.E., University of Waterloo Press, Waterloo, Canada, pp.277-286.

[18] Shinozuka, M., Deodatis, G., and Harada, T. (1987), Digital Simulation of Seismic Ground Motion, *Stochastic Approaches in Earthquake Engineering*, Edited by Lin, Y.K., and Minai, R., Springer-Verlag, pp.252-298.

[19] Somerville, P., Sen, M. and Cohee, B. (1991), Simulation of Strong Ground Motions Recorded during the 1985 Michoacan, Mexico and Valparaiso, Chile Earthquakes, *Bull. of Seism. Soc. of Am., Vol.81*, pp.1-27.

[20] Tajimi, H. (1960), A Statistical Method of Determining the Maximum Response of a Building Structure during a Earthquake, *Proc. of 2nd World Conference on Earthquake Engineering, Vol.2*, pp.781-797.